

**EFFICIENT USE OF COMPONENT MODE SYNTHESIS
USING
IMAGE SUPERLEMENT
APPLIED TO
DYNAMIC ANALYSIS OF
CRANKSHAFT**

by

Minoru Kubota

and

Koji Tanida

Research Institute

Ishikawajima-Harima Heavy Industries Co., Ltd.

Tokyo and Yokohama, Japan

INTRODUCTION

Calculations based on large finite element solid models of actual crankshaft system are indispensable to vibration analysis of the crankshaft system of long-stroke marine diesel engines, but limitations to computer capacity or to computing time preclude analysis by conventional method. The present study covers an attempt at utilizing NASTRAN image superelements and component mode synthesis, with application of the restart function, for analyzing the modal frequency response of pilot and large actual-size models. The computed results are compared with measurements made on actual ship, to verify the functional validity and practical accuracy of NASTRAN applied in this mode. This report presents an illustrative example of analysis applied to a pilot model, undertaken to ensure smooth implementation of full-scale calculations on large actual-size model.

The series of computations using secondary superelement were performed through magnetic tape in the following sequence:-

- 1st run: Eigenvalue analysis of Crank Throw No. 1 on main engine
- 2nd run: Ditto on Crank Throw No. 2 using secondary superelements
- 3rd run: Ditto on complete crankshaft system
- 4th run: Analysis of modal frequency response.

Further, with a view to comparison with the measured results obtained on actual ship, a pilot model was devised appended with propeller shaft and thrust block, with which were performed:-

-5th run: Eigenvalue analysis on overall system

-6th run: Modal frequency analysis on ditto.

Finally, the calculations were made on a large solid model of the actual crankshaft of an IHI-SULZER 6RTA58 type diesel engine, which, together with measured data from actual ship, were compared with the present results, to verify the functional validity and practical accuracy of NASTRAN thus applied.

THEORETICAL EQUATIONS

The generalized equation of motion applicable to a structure modeled by finite element method, upon omitting the damping term, is

$$[M_{ff}]\{\ddot{U}_f\} + [K_{ff}]\{U_f\} = \{P_f\} \quad (1)$$

Rewriting Eq. (1) in terms of the degrees of freedom of the interior and exterior grid points of the superelements,

$$\begin{bmatrix} M_{tt} & M_{to} \\ M_{to}^T & M_{oo} \end{bmatrix} \begin{Bmatrix} \ddot{U}_t \\ \ddot{U}_o \end{Bmatrix} + \begin{bmatrix} K_{tt} & K_{to} \\ K_{to}^T & K_{oo} \end{bmatrix} \begin{Bmatrix} U_t \\ U_o \end{Bmatrix} = \begin{Bmatrix} P_t \\ P_o \end{Bmatrix} \quad (2)$$

where U_o : Degrees of freedom of interior grid points of superelements

U_t : Ditto of exterior grid points of superelements.

We further define

$$\{U_o\} = [G_{ot}]\{U_t\} + [G_{oq}]\{U_q\} \quad (3)$$

where U_q : Degrees of freedom of normalized coordinates. Moreover, in order to determine G_{oq} , we express the overall degrees

of freedom in terms of that referred to normalized coordinates:

$$\begin{Bmatrix} U_q \\ U_t \\ U_o \end{Bmatrix} = \begin{bmatrix} I \\ \phi_{tq} \\ \phi_{oq} \end{bmatrix} \{U_q\} \quad (4)$$

Upon substituting this Eq. (4) into Eq. (3),

$$[G_{oq}] = [\phi_{oq}] - [G_{ot}][\phi_{tq}] \quad (5)$$

Further substituting this Eq. (5) into Eq. (3),

$$\{U_o\} = [G_{ot}]\{U_t\} + ([\phi_{oq}] - [G_{ot}][\phi_{tq}])\{U_q\} \quad (6)$$

where the first and 2nd terms of the right-hand side represent respectively the static and dynamic contributions to the degrees of freedom.

It is to be noted that the above Eq. (6) --- unlike the Guyan reduction* --- includes the dynamic contribution of the 2nd term. If we let the degree of freedom in reference to normalized coordinates equal that eliminated by substitution, the solution will become rigorous**.

Equation (6) twice differentiated gives the acceleration:

$$\{\ddot{U}_o\} = [G_{ot}]\{\ddot{U}_t\} + ([\phi_{ot}] - [G_{ot}][\phi_{tq}])\{\ddot{U}_q\} \quad (7)$$

*) Guyan reduction: Displacement and acceleration of the eliminated interior grid points are respectively

$$U_o = G_{ot} U_t \quad (A-1)$$

$$\dot{U}_o = G_{ot} \dot{U}_t \quad (A-2)$$

With MSC/NASTRAN, the function performed by this Guyan reduction can be utilized instead of the superelement.

**) Rigorous solution: If the normalized coordinates are not adopted, the expression corresponding to Eqs. (A-1) and (A-2) become

$$U_o = G_{ot} U_t + U_o^0 \quad (B-1)$$

$$\dot{U}_o = G_{ot} \dot{U}_t + \dot{U}_o^0 \quad (B-2)$$

where U_o^0 : Displacements of interior grid points that result from constraining the t-set degrees of freedom and applying external loads on the interior grid points.

Using Eqs. (6) and (7), the overall physical degrees of freedom can be transformed to the generalized degrees of freedom --- contracted to the normalized and a limited number of physical coordinates --- through the relations

$$\begin{Bmatrix} U_t \\ U_o \end{Bmatrix} = \begin{bmatrix} O & I \\ G_{oq} & G_{ot} \end{bmatrix} \begin{Bmatrix} U_q \\ U_t \end{Bmatrix} \quad (8)$$

$$\begin{Bmatrix} \ddot{U}_t \\ \ddot{U}_o \end{Bmatrix} = \begin{bmatrix} O & I \\ G_{oq} & G_{ot} \end{bmatrix} \begin{Bmatrix} \ddot{U}_q \\ \ddot{U}_t \end{Bmatrix} \quad (9)$$

The resulting equation of motion in reference to the reduced generalized coordinates, is

$$\begin{bmatrix} O & I \\ G_{oq} & G_{ot} \end{bmatrix}^T \begin{bmatrix} M_{tt} & M_{to} \\ M_{to}^T & M_{oo} \end{bmatrix} \begin{bmatrix} O & I \\ G_{oq} & G_{ot} \end{bmatrix} \begin{Bmatrix} \ddot{U}_q \\ \ddot{U}_t \end{Bmatrix} + \begin{bmatrix} O & I \\ G_{oq} & G_{ot} \end{bmatrix}^T \begin{bmatrix} K_{tt} & K_{to} \\ K_{to}^T & K_{oo} \end{bmatrix} \begin{bmatrix} O & I \\ G_{oq} & G_{ot} \end{bmatrix} \begin{Bmatrix} U_q \\ U_t \end{Bmatrix} = \begin{bmatrix} O & I \\ G_{oq} & G_{ot} \end{bmatrix}^T \begin{Bmatrix} P_t \\ P_o \end{Bmatrix} \quad (10)$$

$$\begin{matrix} \downarrow & & \downarrow & & \downarrow & & \downarrow & & \downarrow \\ [\bar{M}_{aa}] & & \{\ddot{U}_a\} & + & [\bar{K}_{aa}] & & \{\bar{U}_a\} & = & \{\bar{P}_a\} \end{matrix}$$

where

$$\begin{Bmatrix} [\bar{M}_{aa}] \\ [\bar{K}_{aa}] \\ \{\bar{P}_a\} \end{Bmatrix} = \begin{Bmatrix} \begin{bmatrix} G_{oq}^T M_{oo} G_{oq} & G_{oq}^T (M_{to} + G_{ot}^T M_{oo})^T \\ (M_{to} + G_{ot}^T M_{oo}) G_{oq} & M_{tt} + G_{ot}^T M_{to}^T + M_{to} G_{ot} + G_{ot}^T M_{oo} G_{ot} \end{bmatrix} \\ \begin{bmatrix} G_{oq}^T K_{oo} G_{oq} & O \\ O & K_{tt} + K_{to} G_{ot} \end{bmatrix} \\ \begin{Bmatrix} \bar{P}_q \\ \bar{P}_t \end{Bmatrix} = \begin{Bmatrix} G_{oq}^T P_o \\ P_t + G_{ot}^T P_o \end{Bmatrix} \end{Bmatrix}$$

CALCULATION MODELS

The crankshaft subjected to analysis had 6 crank throws --- designated Nos. 1 to 6 --- fired in the order 1-6-2-4-3-5 with crank angles shifted by 60°. The crankshaft is shown in outline in Fig. 1 (a); the corresponding pilot and large solid models are presented in the accompanying diagrams (b) and (c).

What we call the "pilot model" represents all the members of the entire crankshaft in terms of beam elements; "large solid model" represents a single crank throw in finite elements. This latter model was defined in the present instance using the pre-processor program SANA/MESH(1)(2) developed at IHI for general structural analyses. The Pilot Model A --- Fig. 2 --- has the end beams at both extremities extended, one of the extended ends being fixed and the other end free. In this model, the superelements corresponding to the Cranks Nos. 1 to 6 are identified respectively by the symbols 10 to 60.

Eigenvalue analysis with the Pilot Model A was performed in 4 runs, as depicted in Fig. 3:-

- 1st run: On one crank throw only --- that of the Crank Throw No. 1 ("primary" Superelement 10) --- under the virtual boundary condition of one end fixed and the other end free
- 2nd run: The "secondary" Superelement 20 defined; eigenvalue analysis covering 2 crank throws
- 3rd run: Secondary Superelements 30 to 60 defined; entire crankshaft system --- including the end beam extensions (one end fixed, the other free) --- analyzed
- 4th run: Analysis of modal frequency response, with external load applied.

The Pilot Model B --- Fig. 4 --- further incorporates thrust block and propeller shaft, for conducting vibration analyses of the crankshaft system for a diesel-driven ship*.

*) Diesel-propelled ship: The ship envisaged was a 24,300 DWT LPG ship built at IHI, propelled by IHI-Sulzer 6RTA58 engine at 105 rpm maximum continuous and 99.5 rpm normal rating.

The propeller shaft was modeled in terms of beam elements, and the thrust block by scalar spring element; the torsionally and axially vibrating masses of propeller, couplings and flywheel were modeled by lumped moments of inertia and lumped mass, respectively. Further, inertial masses equivalent to the reciprocating parts were added to the crankpins.

Using this model, the analysis proceeded with:-

- 5th run: Eigenvalue analysis of overall shafting system
- 6th run: Analysis of modal frequency response, with external load applied.

ANALYSES USING THE PILOT MODEL A

1st Run --- Eigenvalue Analysis of Primary Superelement

This run on a single crank --- that of the Crank Throw No. 1 (Superelement 10) --- was performed using the model shown in Fig. 5, where the closed circles represent interior, and the open circles exterior, grid points. The external loads act at the exterior grid points numbered 108 to 112, so the elements (108) to (111) were defined by SEELT card in order to incorporate these elements in the Superelement 10.

The virtual boundary conditions adopted were one extremity fixed and the other constrained by pin roller, using the SEBSET and SECSET cards. Designation of this virtual boundary condition is required only for the primary --- and unnecessary for the secondary --- superelements.

Calculations proceeded in the sequence: (1) Generation, assembly and reduction of the Matrixes [K] and [M] for the Superelement 10; (2) eigenvalue analysis under the virtual boundary conditions; (3) storage of the results in the data base DB01, to serve as input for the secondary superelements in the succeeding runs. This was followed by: (4) Generation, assembly and reduction of the matrixes [K] and [M] on the Superelement 0; (5) eigenvalue analysis by inverse power method and normalization by mass.

The resulting Eigenvalue modes are presented in Fig. 6 for the 1st to 5th order vibration modes.

2nd Run --- Eigenvalue Analysis of Secondary Superelements

As shown in Fig. 7, the model represents a system comprising the secondary Superelement 20 added to the primary Superelement 10.

Calculations proceeded in the order:

- (1) Generation/assembly/reduction of the Matrixes [K] and [M] for the Superelement 20
- (2) Ditto for the Superelement 0
- (3) Eigenvalue analysis by inverse power method, and normalization by mass.

3rd Run --- Eigenvalue Analysis of Entire Crankshaft System

Using the Pilot Model A --- with the remaining crank throws (Superelements 30, 40, 50, 60) added, and with the end beams

further extended --- eigenvalue analysis was performed on the system as a whole.

With the Superelements 10 and 20 as already defined, the remaining superelements were defined within case control card, and designated in SUBCASE by SUPER cards, in the order of Superelements 10, 20, 30, 40, 50, 60 and 0, the residual structure 0 serving to designate the boundary conditions and Eigenvalue analysis.

The calculations proceeded in the order:

- (1) Generation/assembly/reduction of the Matrixes [K] and [M] for the Superelements 30, 40, 50 and 60
- (2) Ditto for the Superelement 0
- (3) Eigenvalue analysis by inverse power method; normalization by mass.

The resulting Eigenvalue modes are presented in Fig. 8 for the 1st to 3rd order vibration modes. The modes indicated are:-

- 1st order: 11.78 Hz, axial
- 2nd order: 23.61 Hz, torsional
- 3rd order: 34.29 Hz, axial.

4th Run --- Analysis of Modal Frequency Response

Analysis of the modal frequency response was undertaken on independent crankshaft system, for comparison with results of analysis on overall shafting system of actual ship.

The response analysis was performed through application of external load on the model used in the 3rd Run. The external load was, in this instance, the vibration exciting force generated by the gas pressure in cylinder, which acted on the crankpins with (a) radial component F_R , and (b) tangential component F_Q (see Fig. 3(d)).

The modal frequency responses were analyzed for external loads exerted on the individual superelements representing the different cranks, with damping taken into account on each natural frequency, in the form of modal damping.

The external load was defined within case control card, and specified in SUBCASE by SUPER cards in the order of Superelements 10, 20, 30, 40, 50 and 60, with the application of external force specified by the Superlement 0. For Superelement 0, the case control cards used were DLOAD, FREQ, SDAMP and SPC.

The resulting response curves are reproduced in Fig. 9, where the three upper diagrams represent respectively the X-, Y- and Z-direction components of the modal vibration responses at Grid Point 901 (Fig. 3(d)), and the two lower diagrams the corresponding responses at Grid Point 110 (Fig. 5) for the X-direction (tangential) and Y-direction (radial).

The displacements are seen to rise consistently with frequency in all cases, the range of frequency covered (0.2 - 10.5 Hz) being below the 11.78 Hz of the 1st order natural frequency.

ANALYSES USING THE PILOT MODEL B

5th Run --- Eigenvalue Analysis of Overall Shafting System

With this 5th Run, the overall shafting system was analyzed for eigenvalue. The eigenvalues of individual superelements were analyzed by modified Givens' (MGIV) method.

The superelements on which the eigenvalues were sought were:-

- Primary Superelement 10 of Crank Throw No. 1
- Secondary Superelement 70 of propeller shaft.

The Superelement 10 was analyzed on account of the addition to crankpin of moment of inertia mass equivalent to reciprocating parts.

On the overall shafting system, eigenvalue analysis was performed to cover 5 modes, using inverse power method, with normalization by mass. The results --- as shown in Fig. 10 --- are:-

- | | | | |
|--------------|---------|------------------------------------|--------|
| - 0-th order | 0 Hz | (rigid body mode, by support card) | Mode 1 |
| - 1st order | 6.1 Hz | Torsional, 1 node | Mode 2 |
| - 2nd order | 11.8 Hz | Axial, 0 node | Mode 3 |
| - 3rd order | 28.1 Hz | Axial, 1 node | Mode 4 |
| - 4th order | 31.5 Hz | Torsional, 2 nodes | Mode 5 |

Comparison with direct calculation without use of superelements

With a view to examining the accuracy obtained with the secondary superelements, the results of analysis obtained above were compared with corresponding results from direct calculation covering analysis of the overall structure in a single step.

The results --- partially reproduced in Fig. 11 --- have indicated that, up to the 10th mode, the results almost completely agreed with each other in terms of both natural frequency and mode, thus demonstrating ample accuracy ensured by the method for all practical purposes.

Comparisons with calculation using large solid model and with measured data

Comparisons were made with calculation using large finite element solid model and with sample measurements on actual engine. Results of the calculation and measurements are presented in Fig. 12.

The particular advantage of the present method lies in the substantial economy afforded in computing time, as evidenced by the durations of central processing unit occupation (CPU time) compared in the table below between computations using the present pilot model and large solid model.

(Unit: Sec)

CALCULATION MODEL	SINGLE CRANK THROW	OVERALL SYSTEM
Pilot Model B	113 (114 d.o.f.)	343 (516 d.o.f.)
Large solid model	3,030 (5,760 d.o.f.)	4,562 (6,942 d.o.f.)

6th Run --- Analysis of Modal Frequency Response on Overall Shafting System

Following the procedure outlined earlier for the Pilot Model A, analysis of modal frequency response was performed on the overall shafting system, with application of external load.

The resulting response of displacement is reproduced in Fig. 13, which clearly reveals a peak at 6.1 Hz for 1st order torsional vibration.

CONCLUDING REMARKS

Application of component mode synthesis with NASTRAN image superlements as tools for calculation proved to permit for the first time amply accurate derivation of the coupled axial and torsional vibrations of actual crankshaft systems.

The foregoing study definitely demonstrated vibration analyses by means of component mode synthesis using secondary superlements to be practically applicable. Comparisons with calculation using large solid model and with measured data, taking as example an IHI-SULZER 6RTA58 diesel engine, proved ample accuracy to be ensured for deriving both eigenvalues and modal frequency reponses, using the modelization procedure proposed in this report.

Adoption of pilot model eliminated all trouble arising from mismanipulation or error liable to occur in computations using large solid models.

The present method ensures effective saving of computing time, which is particularly significant when compared with computation using solid model of actual crankshaft system. It was also ascertained that restarting is possible even with large models, through the use of multiple tapes.

It is worth recalling that the generation of input data for computations based on solid models of the actual crankshaft system was performed using the pre-processor program SANA/MESH developed at IHI for general structural analyses, and which permitted substantial saving of work required for the inputting operation, while at the same time minimizing the risk of erroneous input.

REFERENCES

- (1) T. Yuki, Y. Yamazaki and Kazuo Otomo, "Data Structure for Structural analysis and Its Application" Ishikawajima-Harima Engineering Review (Japanese language edition), Vol. 24, No. 1 (Jan. 1984)
- (2) T. Yuki, Y. Yamazaki, K. Ohtomo, S. Kato, M. Takada and M. Koyama, "Preprocessor for Structural Analysis: SANA/MESH", Ishikawajima-Harima Engineering Review (Japanese language edition), Vol. 24, No. 5 (Sept. 1984)

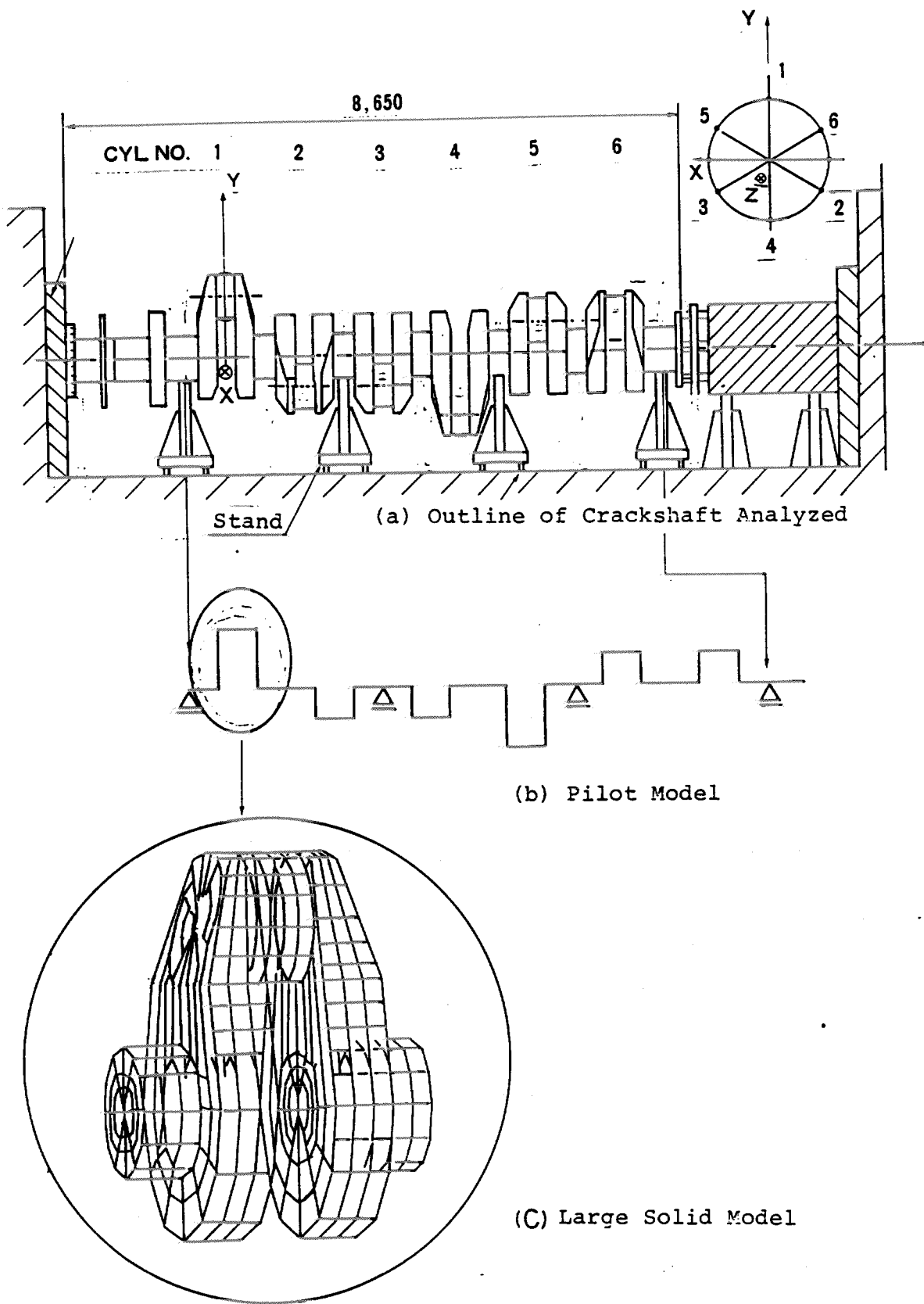


FIG. 1 Crankshaft Subjected to Analysis; Corresponding Pilot and Large Solid Models

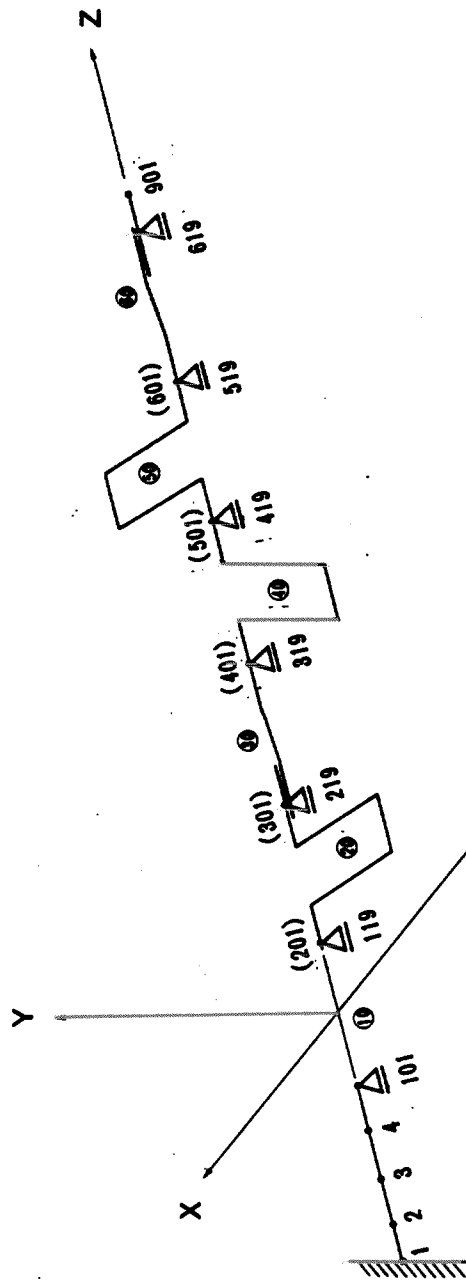
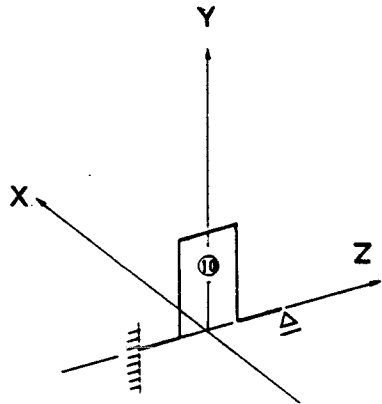
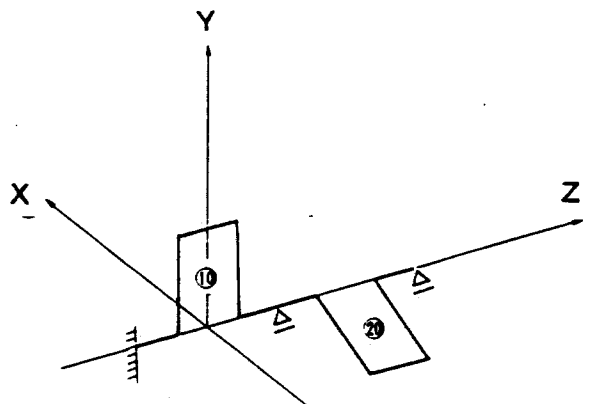


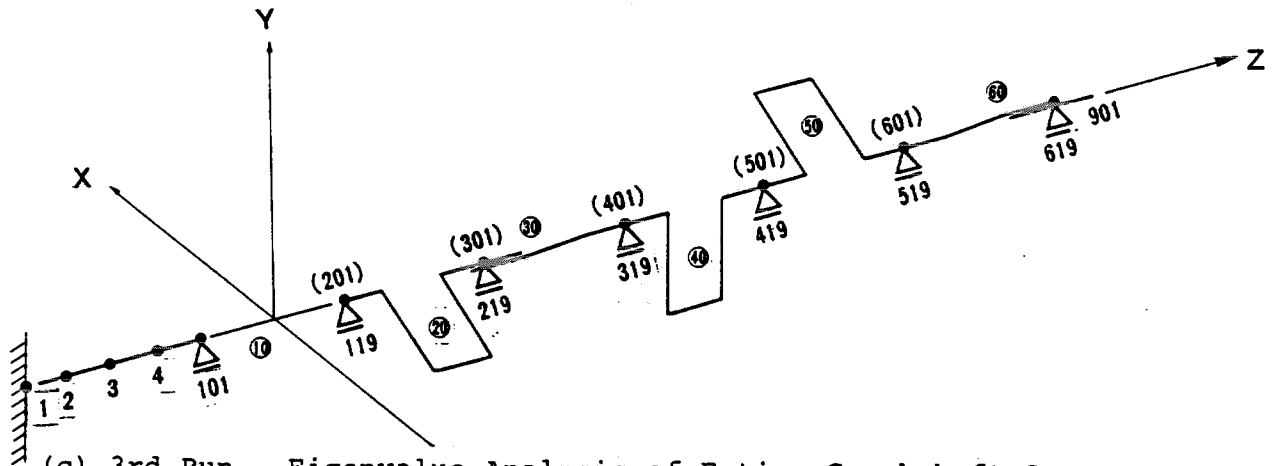
FIG. 2 Pilot Model A



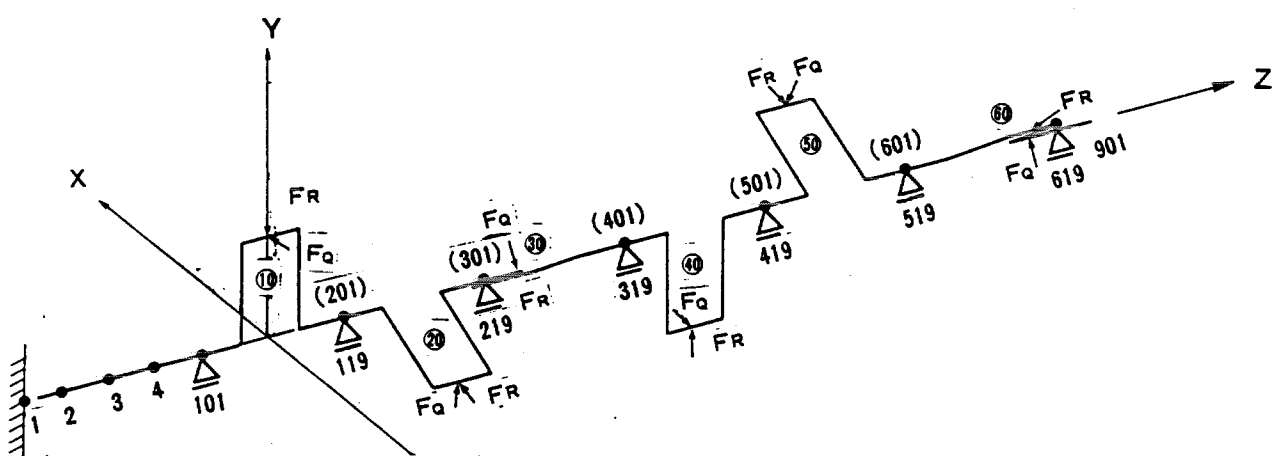
(a) 1st Run - Eigenvalue Analysis of Primary Element



(b) 2nd Run - Eigenvalue Analysis of Secondary Element



(c) 3rd Run - Eigenvalue Analysis of Entire Crankshaft System



(d) 4th Run - Modal Frequency Response Analysis of Entire Crankshaft System

FIG. 3 Versions of Model A Used for 1st to 4th Runs

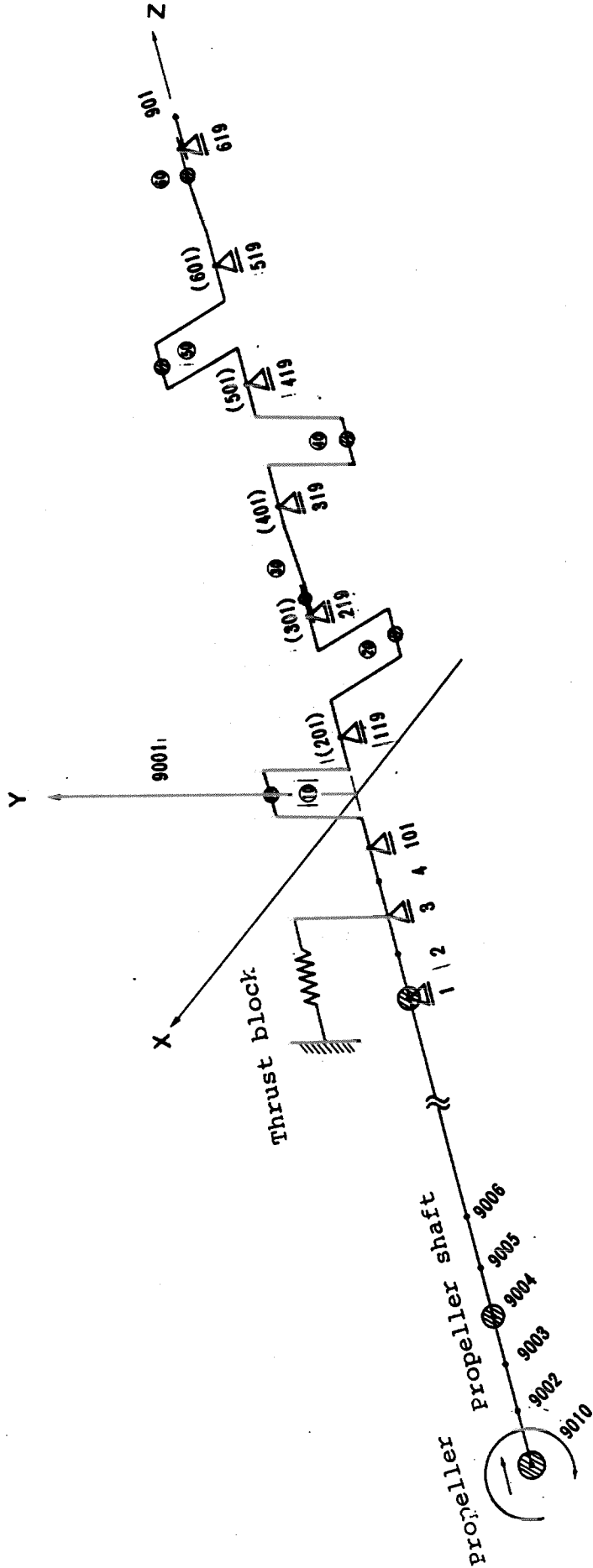


FIG. 4 Pilot Model B

Grid Point Nos.

- : Interior grid point
- : Exterior grid point

Element Nos. ○

boundary condition:-

- One end fixed (SPC1) 101
- Other end constrained by pin roller (SPC1) 119

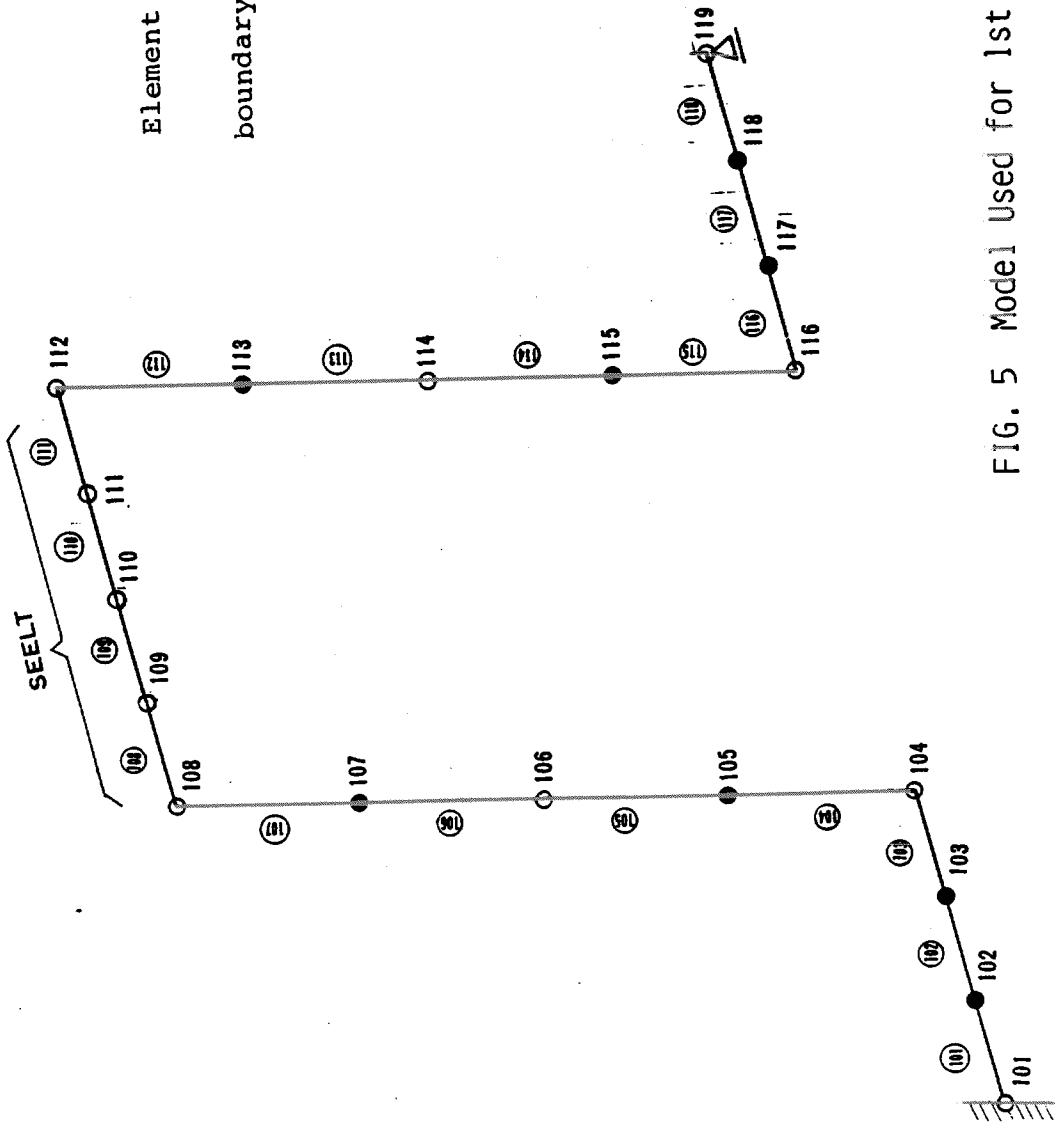


FIG. 5 Model Used for 1st Run with Pilot Model A

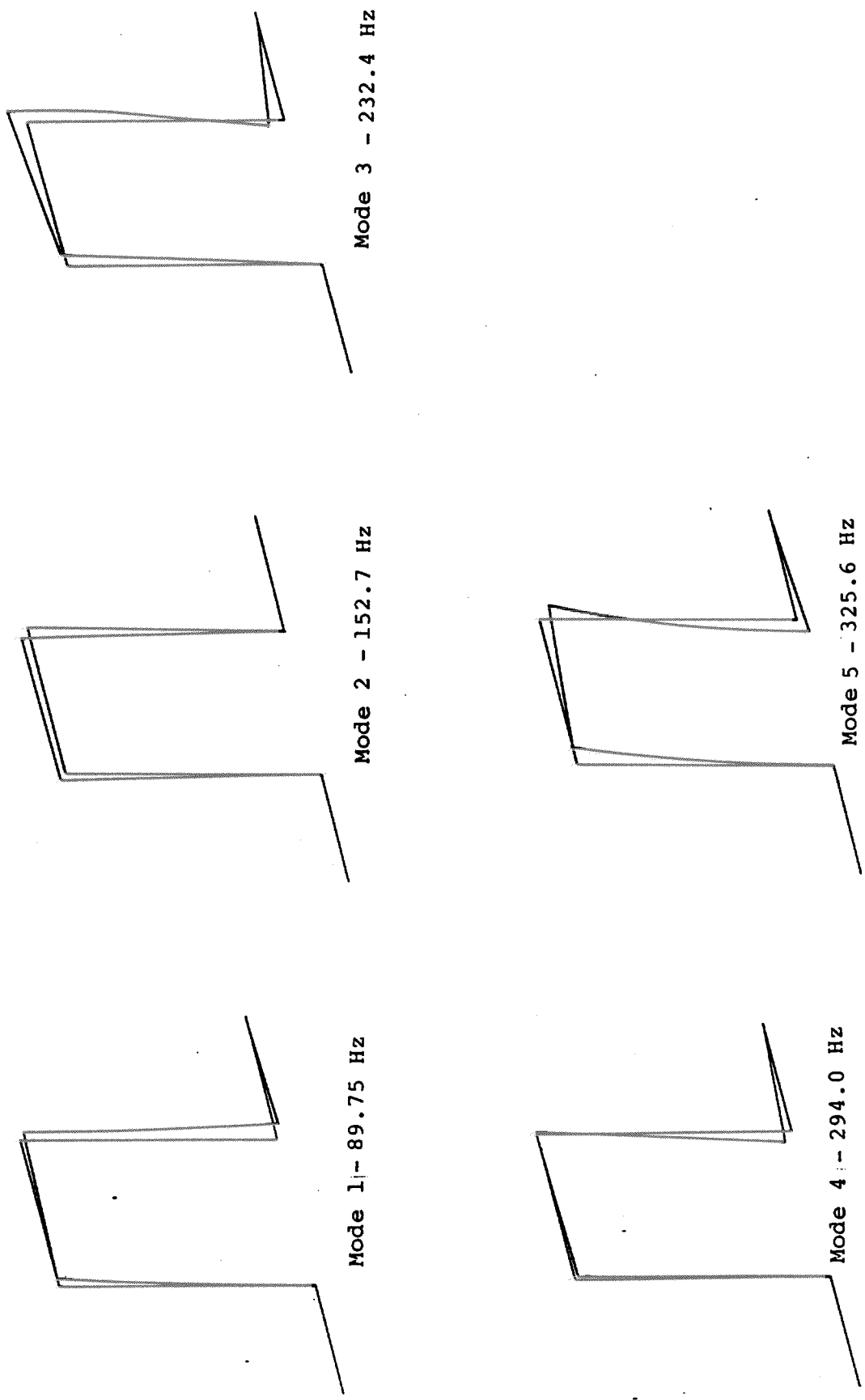


FIG. 6 Eigenvalue Modes Obtained on Primary Superelement

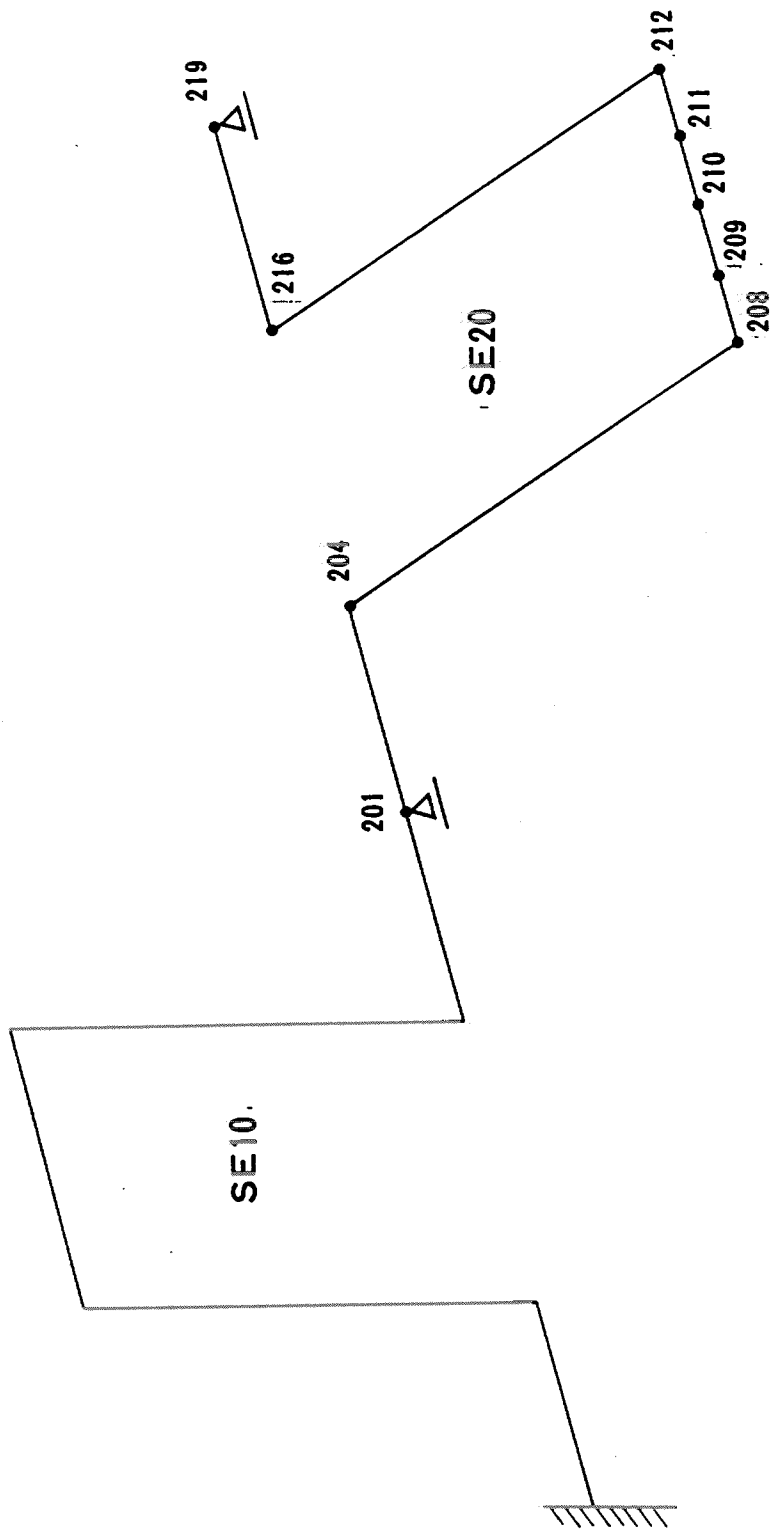
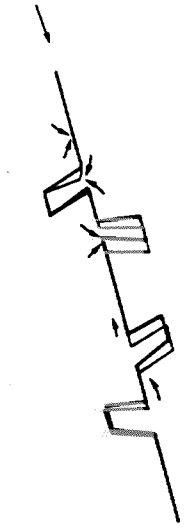


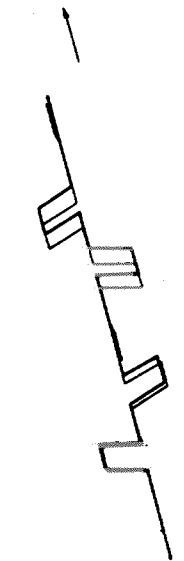
FIG. 7 Model Used for 2nd Run with Pilot Model A



Mode 1 - 11.78 Hz

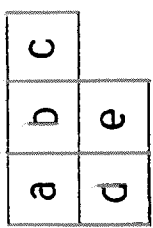
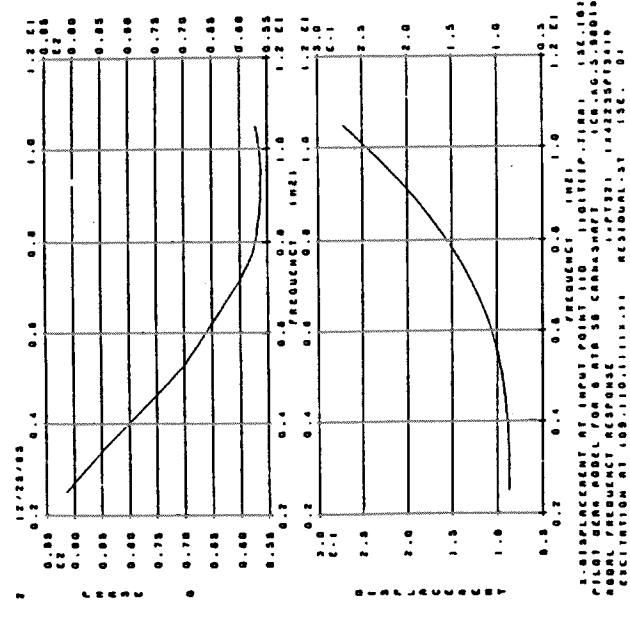
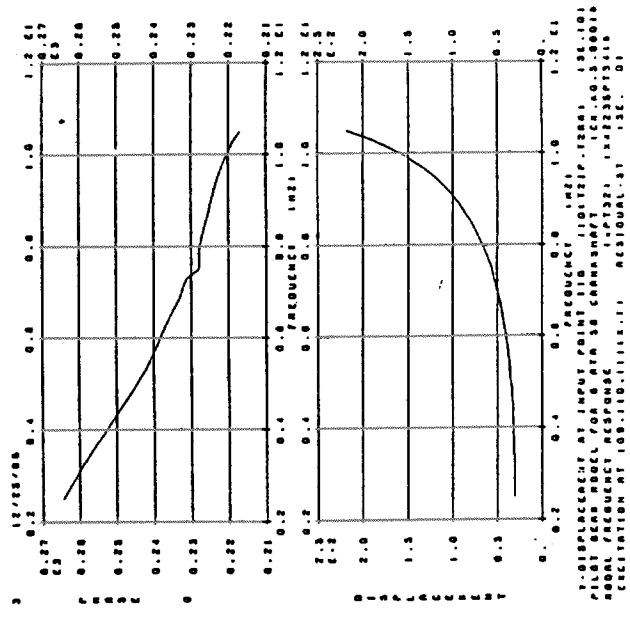
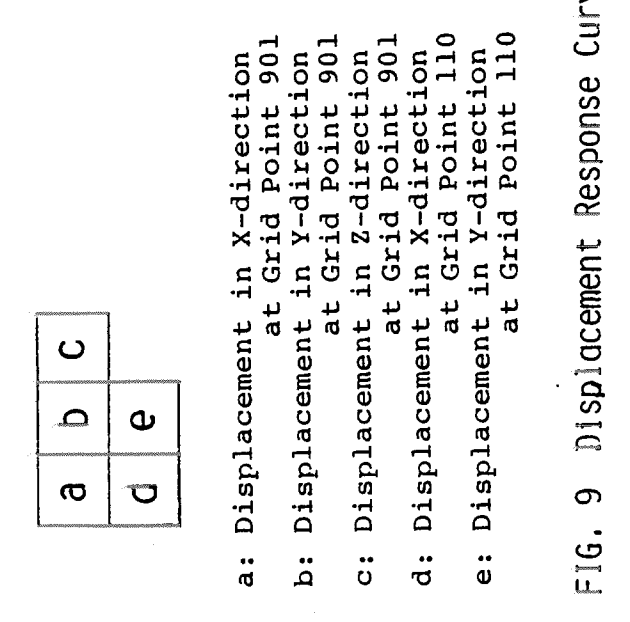
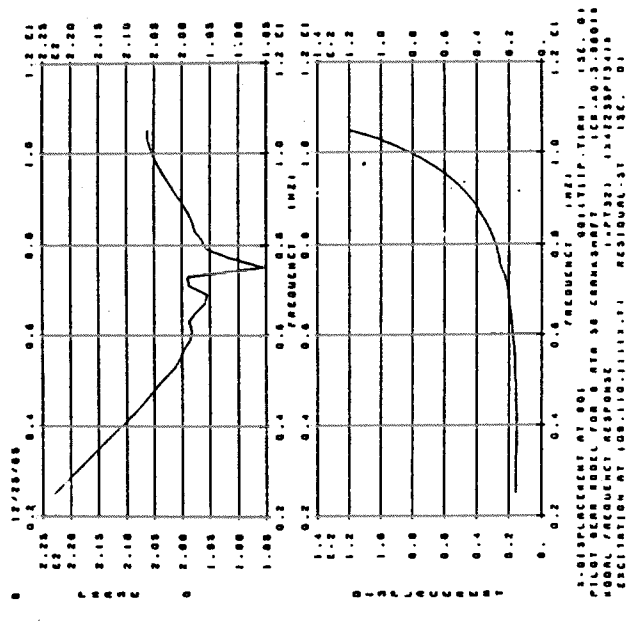
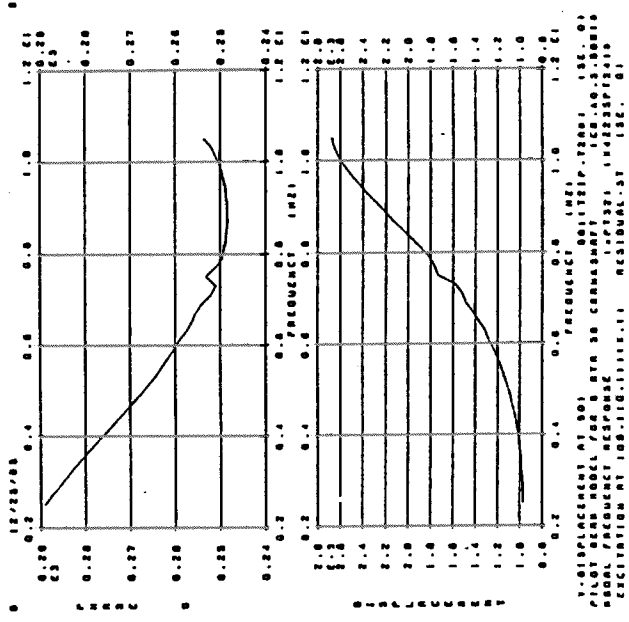
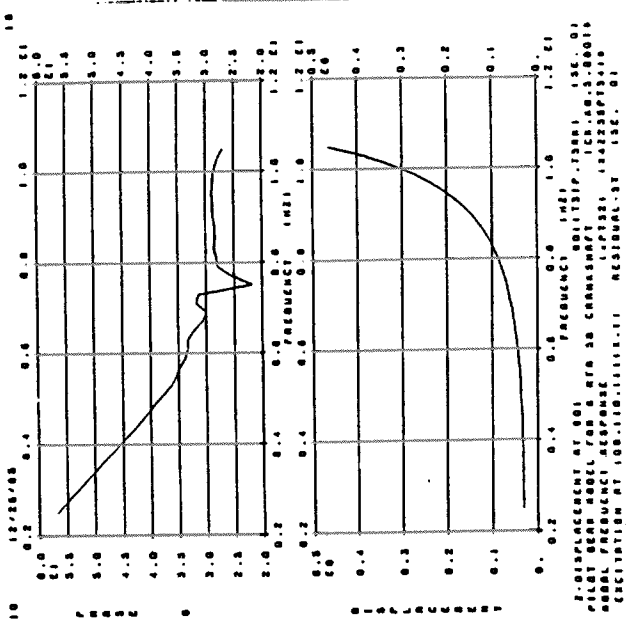


Mode 2 - 23.61 Hz



Mode 3 - 34.29 Hz

FIG. 8 Eigenvalue Modes Obtained on Entire Crankshaft System Using Pilot Model A



- a: Displacement in X-direction at Grid Point 901
- b: Displacement in Y-direction at Grid Point 901
- c: Displacement in Z-direction at Grid Point 901
- d: Displacement in X-direction at Grid Point 110
- e: Displacement in Y-direction at Grid Point 110

FIG. 9 Displacement Response Curves

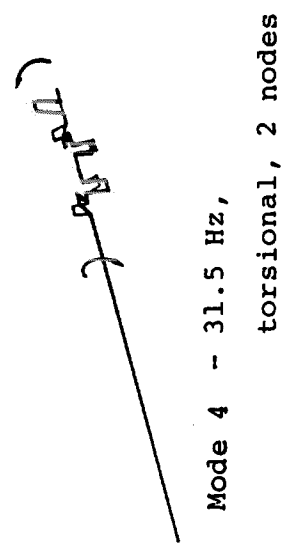
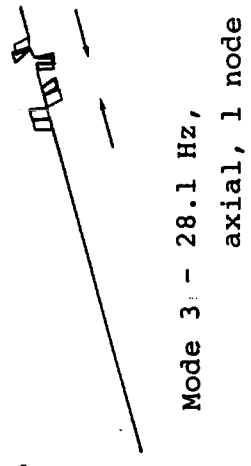
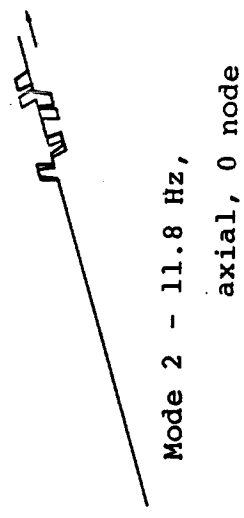
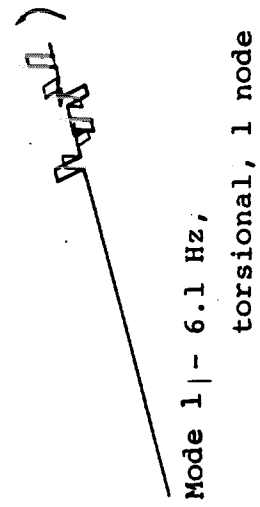
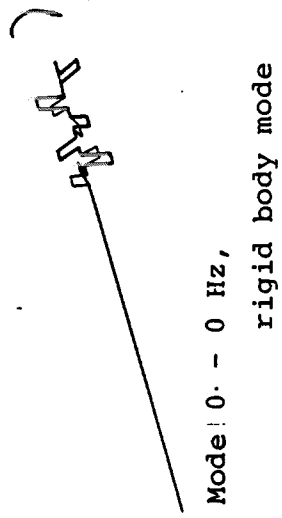
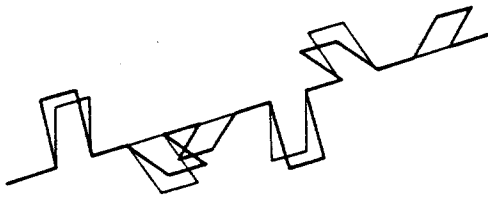
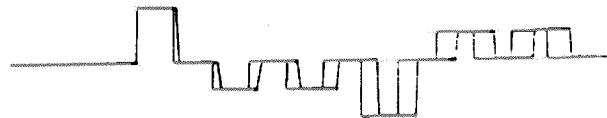
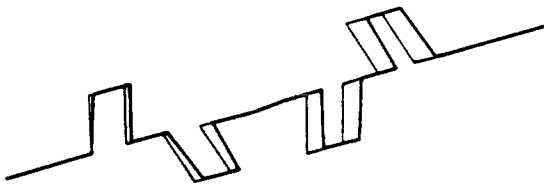


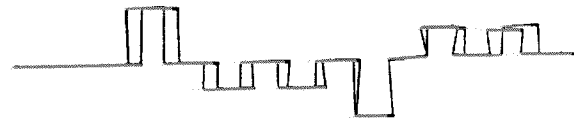
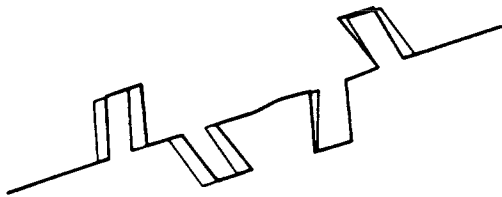
FIG. 10 Eigenvalue Modes Obtained using Pilot Model B



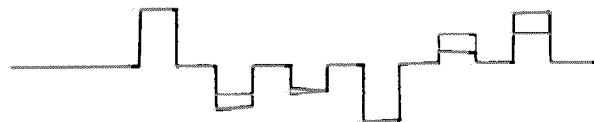
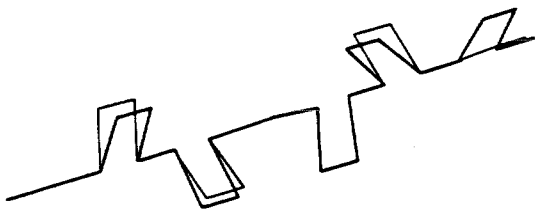
Mode 1 - torsional, 1 node : $f = 6.134$ Hz by component mode synthesis
 $= 6.134$ Hz by direct calculation



Mode 2 - axial, 0 node : $f = 11.78$ Hz by component mode synthesis
 $= 11.78$ Hz by direct calculation

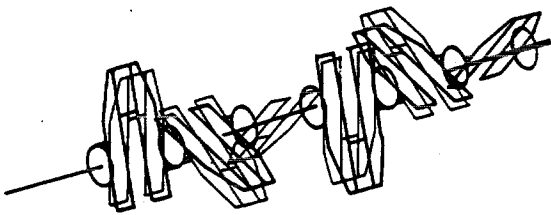


Mode 3 - axial, 1 node : $f = 28.12$ Hz by component mode synthesis
 $= 28.12$ Hz by direct calculation

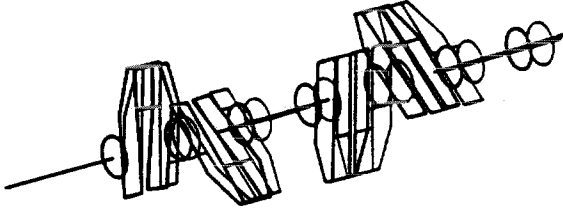
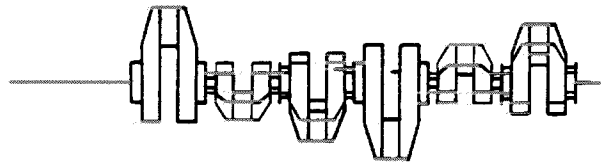


Mode 4 - torsional, 2 nodes : $f = 31.46$ Hz by component mode synthesis
 $= 31.46$ Hz by direct calculation

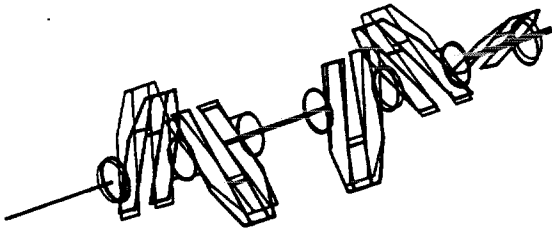
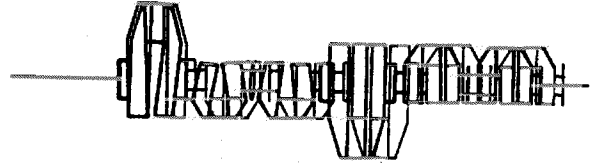
FIG. 11 Comparison of Results Obtained on Crankshaft System
 between Component Mode Synthesis and Direct Calculation



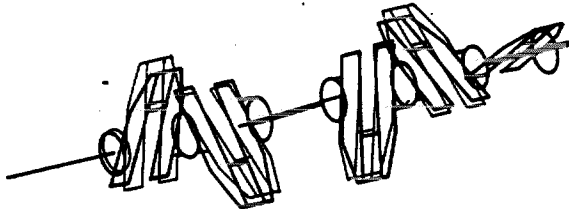
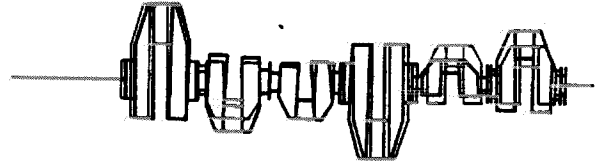
Mode 1 - torsional, 1 node : $f = 5.906$ Hz by solid model
 $= 6.0$ Hz by measurement



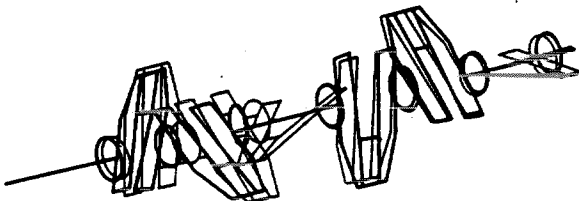
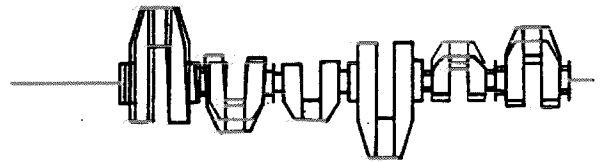
Mode 2 - axial, 0 node : $f = 16.81$ Hz by solid model
 $= 14.6$ Hz by measurement



Mode 3 - axial, 1 node : $f = 30.45$ Hz by solid model



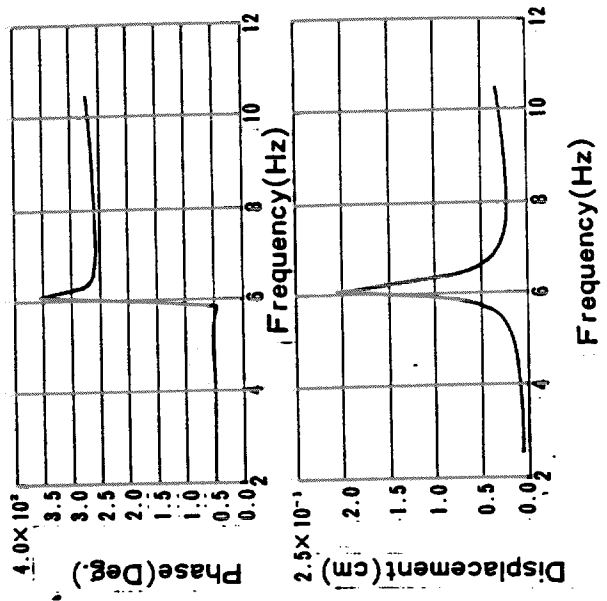
Mode 4 - torsional, 2 nodes : $f = 35.23$ Hz by solid model



Mode 5 : $f = 72.41$ Hz by solid model



FIG. 12 Results Obtained with Large Solid Model and from Measurement



a	b	c
d	e	

- a: Displacement in X-direction at Grid Point 901
- b: Displacement in Y-direction at Grid Point 901
- c: Displacement in Z-direction at Grid Point 901
- d: Displacement in X-direction at Grid Point 110
- e: Displacement in Y-direction at Grid Point 110

FIG. 13 Displacement Response Curves (Obtained for Overall Shafting) System

